IET Image Processing

Research Article

IET Journals
The Institution of Engineering and Technology

Identification of wool and mohair fibres with texture feature extraction and deep learning

ISSN 1751-9659
Received on 16th July 2019
Revised 17th October 2019
Accepted on 7th November 2019
E-First on 6th January 2020
doi: 10.1049/iet-ipr.2019.0907
www.ietdl.org

Kazim Yildiz[1] ✉

[1]*Department of Computer Engineering, Marmara University, Technology Faculty Goztepe, Istanbul, Turkey*
✉ *E-mail: kazim.yildiz@marmara.edu.tr*

Abstract: Wool and mohair fibres are both animal-based fibres and having circular scales on their microscopic images from the longitudinal view. Although they look very similar in their microscopic view, they show different physical/chemical properties which determine their usage area. Thus, in textile industry, they need to be separated carefully from each other. The separation of wool/mohair fibres is an important issue and can be performed with human eye by using the microscopic images, that is not time/cost effective and not objective. The novelty of the presented study is to design an objective, easy, rapid, time and cost-effective method in order to separate wool fibre from mohair fibre by using a texture analysis based identification method. For this purpose, microscopic images of both wool and mohair fibres were preprocessed as the texture images. Local binary pattern-based feature extraction process and deep learning were separately used to get determinative information from the fibres. In order to identify the samples, the classification based method was completed. Experimental results indicated that an accurate texture analysis for this kind of animal fibres is possible to identify wool and mohair fibres by using deep learning and machine learning with 99.8% and 90.25% accuracy rates, respectively.

1 Introduction

Although a number of techniques have been developed in the wool industry, the exact classification of animal fibres is very hard. Some techniques, which use the microscopy with human eye, separate these fibres from the samples of their circular scales and others from their chemical and physical characteristics. However, the characteristic features of these samples are still the most useful proof for the capable microscopy to characterize animal fibres such as wool, merino, mohair and cashmere [1–5]. From this perspective, classification of animal fibres is actually a distinctive task of classification and pattern recognition. Thus, the identification of mohair and wool becomes necessity in manufacturing. There are several methods which are scanning electron microscopy [6], optical microscopy [2, 4], DNA analysis [7], near-infrared (NIR) spectroscopy [8], dyeing methods [9]. Some limitations such as all these systems require high-cost investments, and they are all human based that means the evaluation process cannot be performed objectively.

Recently, in order to build up a practical method for identification and classification of the animal fibres, image processing technique is used to extract significant knowledge from samples and linear functions to categorize merino and cashmere fibres based on a linear discriminant statistical analysis in Robson's study [10]. A non-linear artificial neural network (NANN) used to characterize mohair and merino with a non-linear discrimination function instead of linear discrimination function. Results proved that the non-linear discrimination function was better during the characterization process of mohair and merino [11]. In order to classify the animal-based fibres, fuzzy-based pattern recognition has been used [12]. A mohair and merino fibres are classified with fuzzy neural pattern recognition. With the unsupervised network two multilayer networks have been used. To extract the features, the supervised network rendering as the classifier established on the features then unsupervised network. The experimental results showed that hybrid network has an ability to exactly characterize the two fibres. Zhong *et al.* have used three different decoding methods which are direct geometrical description, recurrence quantification analysis and discrete wavelet transform with the embedded features. The features have been used to monitor the supervised classification methods which are kernel ridge regression/classification, support vector machine (SVM) and a neural network with multilayer perceptron (MLP). Results proved that the designed projection curves could be used in automatic cashmere/wool identification [13]. She *et al.* presented a novel method which uses the non-linear demarcation functions with an artificial neural network (ANN). The feature patterns have been obtained with the help of image processing. The ANN model has been used for classifying mohair and merino fibres [11]. Xing *et al*. [14] have developed a micro-analysis system to digitalize the animal fibres. The proposed method has been designed based on Wavelet and Markov random filed. Accordingly, the system identifies the cashmere, sheep wool and goat hair. Xing *et al.* have used grey level co-occurrence matrix algorithm to extract features and the diameter of fibres has been measured by interactive measurement algorithm. For classification process, *K*-means algorithm has been used and the recognition rate has been found as 94.29% [15]. Zhang *et al.* [16] presented wavelet transform based extraction process for fibre texture features for classifying superfine merino wool and cashmere fibres. The proposed system has enabled to develop automatic identification for animal-based fibres. Novel identification algorithms based on *K*-mean clustering, parallel algorithm and fractal algorithm have been all proposed. The experimental results proved that the proposed method was feasible to measure and classify the wool and cashmere fibres [17]. In another study, Zhang *et al*. have been proposed a novel representation learning model. It was able to extract the adaptive locality-preserving salient features. The experimental results showed that the proposed method, robust block diagonal adaptive locality-constrained latent representation was better than the other state of the art methods [18]. Kong *et al.* [19] have presented two different model-based applications to extract features. In the first model, the pre-designed features have been used and in the second one an unsupervised ANN has been used to extract the most determinative and global features from the animal fibre images. In a previous study, Zhang *et al*. have proposed a two-dimensional (2D) neighbourhood preserving projection to extract the features of 2D images. The method was preserving features to minimize the reconstruction error which is sensitive for outliers in data. The methods showed better results compared to the state of the art [20]. Zhang and colleagues have discussed an enhanced robust representation and classification method. It was found to be more

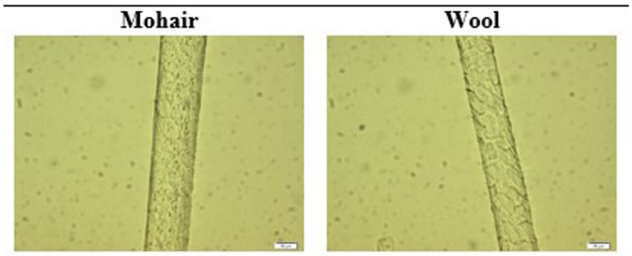

Fig. 1 *Microscopic images of mohair and wool fibres*

powerful and had information features from data for representation. The results showed that the proposed method outperforms for representation and classification [21]. Shi and You have developed a learning vector quantization model to differentiate the cashmere and fine wool animal fibres. The images of fibres have been processed and four main parameters from their skeletonized binary level extracted as feature. The correspondence results showed that the proposed model is more understandable and definite [22]. There are so many application areas with local binary pattern (LBP) histogram which are face analysis, texture classification, video background subtraction, and region of interest [23–31]. Although all these works present various image processing-based solutions regarding identification of animal-based fibres, this paper differs from the other literature works by being more descriptive, using the local-based feature extraction method, and showing the highest performance of the accuracy rate. Additionally, this paper uses deep-learning-based application which can be accepted as a comparative study.

In this paper in order to perform mohair and wool classification process with a practical and scientific way, a characterization process on texture features was proposed. The microscopic samples are obtained by Olympus microscope, and then preprocessed in order to be analysed by LBP. Characteristic LBP parameters of texture feature were collected. These features are used as an input for nearest neighbour (NN) classification with chi-square distance. The second way, deep learning is used to identify the mohair and wool fibres. With this proposed model, characterization process can be performed automatically.

2 Material and methodology

2.1 Microscopic images of materials

The surface photographs of wool and mohair fibres were captured by using the Olympus BX51 microscope (Fig. 1). From different regions of microscopic surface topography of fibres, 50 different images in original size (2080 × 1544 pixels) were captured. The presence of the data zone restricted the useful area to 2080 × 1460. The similarity between two animal fibres can be seen in Fig. 1 with magnification rate × 100. Mohair and wool fibres are both categories of animal-based fibre but they differ from their animal type. Mohair fibre belongs to Angora goat whilst wool fibre is obtained from sheep. The cortex of both wool and mohair fibre is surrounded by a cuticle of flatted cells that is noted as scales like other animal fibres which are overlapping one another. In some applications for their identification and classification, the form and order of the cuticle scales form distinctive patterns, allowing for differentiation.

Fig. 1 shows the light microscopy images of mohair and wool fibres from their longitudinal way, respectively. During the experimental process, 50 mohair and 50 wool images were captured by the microscope. One mohair and two wool samples were excluded from the main data set due to the quality of images. Thus, totally 97 images (49 mohair and 48 wool) were used in experimental part.

2.2 Preprocessing of images

Both mohair and wool fibres are preprocessed before the feature extraction process. The background information is unnecessary for the extraction. Fig. 2, the original grey image from figure, the grey level pixel value is very tight to the target fibre's but the information is needed only from the fibre surface rather than the whole image. Thus, to overcome the effect of background, the fibre subtraction process is applied. There, binarisation threshold is used to get a boundary.

First, image was converted into greyscale. Grey-level image was converted to binary image by thresholding. The binary image was converted into its complement. In order to fill the small holes, dilation and erosion (closing process) were implemented with certain same sized ellipse-shaped structuring element. Then to remove the small size of parts, opening process was implemented with particular size of cross-shape structuring element. Desired object coordinates were taken from opened image and with the help of bitwise and operation same coordinates extracted from initial greyscale image. Unnecessary parts for feature extraction were eliminated from the image.

In order to extend the data set, with the help of the OpenCV library, 18 new images were generated for each fibre microscopy image. In the initial phase, resolution of each image was 2080 × 1544 pixel, respectively. During preprocessing operation width of the image may change but height stays as its initial value. So, each image height was set as 1544 pixel. By using this advantage each image was cropped into three parts as their height value was 514-pixel length. Fig. 2 shows the preprocessing procedure of the image.

Then five additional operations which are (i) horizontal flipping, (ii) vertical flipping, (iii) transpose of image matrix, (iv) horizontal flipping of transposed image, (v) vertical flipping of transposed image, were all performed on each cropped image (Fig. 3). Fig. 3 shows the additional operations on the image. As a result, 18 images were generated from one fibre image.

2.3 Feature extraction

In this study, LBP was employed as feature extraction. The detailed information about the methods is given below.

2.3.1 Local binary pattern: The identification of the fibre using the feature characteristics of the fibre image can be defined as the pattern recognition task. The main idea about this function is to remove significant information from fibre samples. Among the feature extraction methods, LBP is a substantial procedure because of low computational cost and high discriminative feature characteristics.

In basic LBP, eight neighbours of each pixel is compared. Each element is subtracted from the centre pixel value. Then obtained negative values are defined as 0 and the positives are with 1. A binary number is entered in a clockwise direction beginning from the top-left. The corresponding decimal value is obtained from this binary value. It is illustrated in Fig. 4.

LBP was operated to extract the local features and proposed by Ojala *et al.* [23]. For representing the whole image, a statistical histogram of local patterns were generated. Let T be a texture with grey levels of P ($P > 1$) image pixels as

$$T \simeq t(s(g_o - g_c), s(g_1 - g_c), \ldots, s(g_{P-1} - g_c)) \quad (1)$$

Given the intensity value g_c of a centre pixel and its P circularly and neighbours $g_{p,R}$ with radius R where $p = 0, 1, P$; LBPs were defined as

$$\mathrm{LBP}_{P,R} = \sum_{p=0}^{P-1} s(g_{p,R} - g_c)2^p \tag{2}$$

where s is a sign function generating 1 for a non-negative value and otherwise its value is 0 as shown below

$$S(x) = \begin{cases} 1, & x \geq 0 \\ 0, & x < 0 \end{cases} \tag{3}$$

The main difficulty of the basic LBP is looking for 3×3 neighbourhood. It cannot obtain influential features with the major scale. To overcome this, the operator was generalized [24]. A series of sampling points define a local neighbourhood, which are placed at equal intervals in a circle centred on the pixel to be labelled. The sampling points do not fall within the pixels interpolated using bilinear interpolation because of permitting any radius. Fig. 5 illustrates the extended LBP operator where P is determined as sampling points on circle of radius R.

In texture classification, a unique identifier was assigned for binary codes with the same circularly modified shape and show rotation invariant $\mathrm{LBP}_{P,R}$as $\mathrm{LBP}^{\mathrm{ri}}_{P,R}$, where ri represents rotation invariance to guarantee the rotation invariance [23]. The uniform pattern, showed as '$u2$', is widely used for checking the frequency of bitwise changes from 0 to 1 or 1 to 0 for reducing the future dimension. The mapping from a binary pattern to a decimal feature value is shown based on the 'riu2' grouping strategy as follows:

$$\mathrm{LBP}^{\mathrm{riu2}}_{P,R} = \begin{cases} \sum_{p=0}^{P-1} s_{p,R}, & U(\mathrm{LBP}^{\mathrm{ri}}_{P,R}) \leq 2 \\ P+1, & \text{Otherwise} \end{cases} \tag{4}$$

In (4), where 'riu2' superscript indicates that the pattern contains uniform mapping, rotation invariance and function $U(.)$ which count the frequency of bitwise transitions.

2.4 Classification

On the strength of the LBP histogram of texture samples, the texture classification with rotation invariance can be implemented. For this purpose, the NN classifier was used. The detailed information about the algorithm was given below.

2.4.1 Nearest neighbour: In this study, we mainly discuss on deep-learning architecture rather than classifier, so we use the simplest classifier to distinguish features. For measuring the similarity of histograms M and T in order to test image I_{T} and model image I_{M}, the NN classifier was used the distance method as chi-square [11] as

$$D(T,M) = \sum_{n=1}^{N} \frac{(T_N - M_N)^2}{T_N + M_N} \tag{5}$$

N determines the number of bins, at the nth bin T_n and M_n are the values of T and M. I_{T} is a test image which is assigned to the class of I_{M}. The minimal chi-square distance is related to I_{M}.

2.5 Deep learning architecture

Deep learning algorithms originate from ANNs. If the number of hidden layers exceeds five in ANNs, the complexity increases and the situation cannot be improved. Deep learning architectures are multilayered and contain many parameters. The mainly used architecture is a convolutional neural network (CNN). In the next section, the architecture of CNN will be discussed.

2.5.1 Convolutional neural network: It was proposed by LeCun *et al*. in 1998 [32]. The idea that LeCun and his team practiced was older, they developed their ideas on the seminar paper, which was presented in the year of 1968 by Hubel and Weisel [33]. It defines a

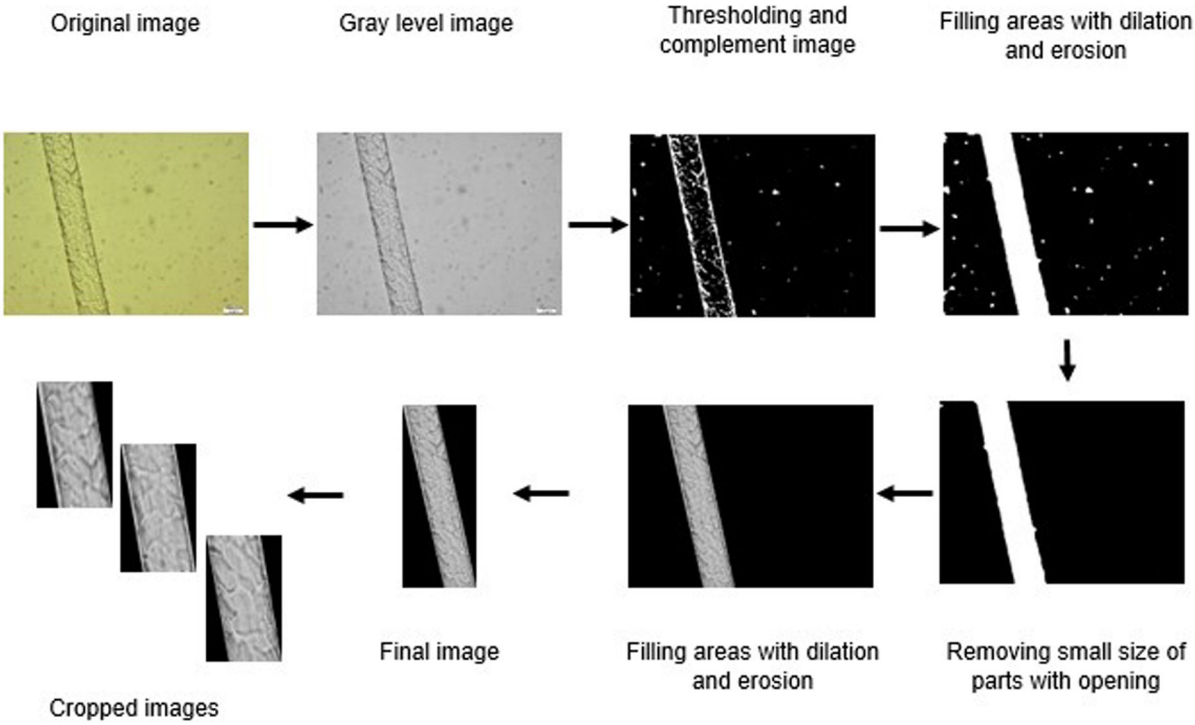

Fig. 2 *Preprocessing procedure of the image*

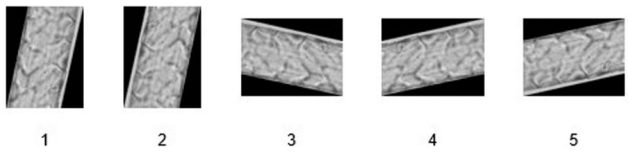

Fig. 3 *Additional operations on each cropped image*

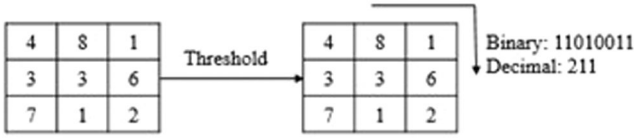

Fig. 4 *Example of LBP operator basically*

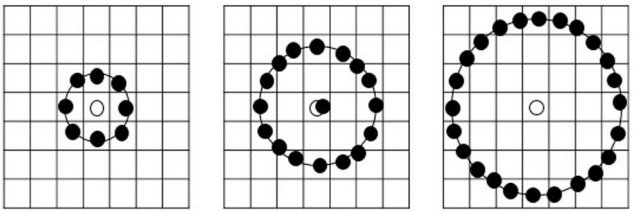

Fig. 5 *Example of the extended LBP [24]: (8, 1), (16, 2), (24, 3)*

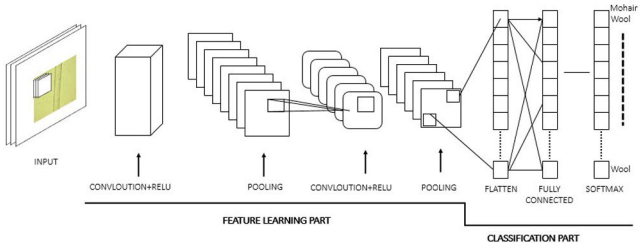

Fig. 6 *Proposed CNN architecture*

Table 1 Classification results with LBP and NN

(Radius, points)		Accuracy					Average accuracy, %
Training samples, %	Testing samples, %	(1, 8)	(2, 16)	(3, 16)	(2, 24)	(3, 24)	
10	90	70, 33	72, 44	85, 00	70, 33	84, 11	76, 44
20	80	72, 25	79, 12	93, 25	72, 62	92, 00	81, 84
30	70	78, 63	82, 85	94, 57	76, 14	95, 71	85, 58
40	60	75, 99	88, 66	94, 83	86, 50	95, 83	88, 36
50	50	78, 60	90, 20	96, 20	87, 60	97, 20	89, 96
60	40	79, 50	90, 25	98, 25	87, 00	96, 25	90, 25

feed-forward neural network and is commonly used in image analysis. CNN's have three main parts: convolutional, pool and completely bound layer. The convolutional layer implements a series of filters to the local fields of the input, thereby getting property maps of the input image [34]. The convolution of x_s given filter i is calculated as

$$f_{i,s} = \sigma(W^i x_s + b^i) \tag{6}$$

where the number of filters should be k and $M \times N$ determines the size of the input image, b^i is the bias of filter i, x_s is the small patch, W^i is the weight of filter i, σ is the activation function. The convolutional output is calculated as

$$k \times \left\lceil \left[\frac{(M-a+1)}{s} \right] \right\rceil \times \left\lceil \left[\left(\frac{N-b+1}{s} \right) \right] \right\rceil \tag{7}$$

with size, where $\lceil . \rceil$ is a ceiling function in (7).

The pooling layer applies the sampling through the spatial dimensions of the input. Equation (8) shows the max-pooling of image patch x_s

$$\text{pool}_s = \max(x_s) \tag{8}$$

After the convolution layer, the pooling layer was applied because of the size of features and to overcome of over-fitting. For example max pooling with patch size $c \times d$ and input size $M \times N$ produces output as in (9) for size.

$$\lceil [(M - 1/c)] \rceil \times \lceil [(N - 1/d)] \rceil \tag{9}$$

The fully interconnected layers form the last few layers of a CNN and calculate class scores. A deep CNN comprises of pooling varying convolutional layers, which are maintained by completely bound layers. CNN structure was commonly used in computer vision tasks like video and scene analysis and object recognition [35–38].

Fig. 6 shows the used architecture of CNN. Model retrained with the pre-trained model of Google's open-source library Tensorflow which is Inception V3 model. This model trained by Tensorflow with the ImageNet data set. Generally, CNN model architecture is separated into two parts which are feature learning and classification. In feature learning part, by convolving filter matrix on each image matrix certain features are extracted, then to ensure the non-linearity in convolutional network ReLU activation function is used. Then in order to reduce the feature map parameters pooling process is implemented. According to the particular purposes max, average, and sum pooling operations should be processed. This process is continuing with the different filter matrixes like 1×1, 3×3, and 5×5. At the classification step, feature matrix is flattened into feature vector and feed into fully connected layer. Then, as a result Softmax is used as an activation function to classify the output.

So, with the help of transfer learning technique, the last layer of CNN model retrained again with the data set. For classification, Tensorflow's Inception CNN model uses Softmax function after fully connected layer (Fig. 6). At the initial stage of the re-training process, the designed network was fed with provided 97 images (49 mohair and 48 wool) only by applying the background elimination process on them. This approach showed promising results as images did not contain useless background data, but this result was not sufficient. The reason for the low accuracy result was the insufficient number of images. In order to overcome this problem, data augmentation techniques were applied on images to increase the number of images artificially and to create synthetic data set from existing low number of data. With the help of flipping and scaling techniques of data augmentation, the data size was increased 18 times as mentioned in Figs. 2 and 3. Chosen techniques (flipping and scaling) were the most relevant ones for this case rather than translation, rotation, adding noise and light adjustment techniques. The flipping and scaling images increase the variety, whereas others add no value to the data set. After data augmentation process, re-training process was repeated again and at this time the accuracy rates were increased fairly.

3 Results and discussion

In order to evaluate the performance of the proposed methods, feature extraction method was applied to microscope images which contain two classes of texture images for animal fibres. Test and training data sets were selected randomly and tried them ten times of texture images. Under each condition, each set contains 50 non-overlapping instances. The experimental procedure was given as follows in detail.

In order to test, all samples were captured with the same condition and separated as training and testing sets for the evaluation procedure. Training and testing samples were selected randomly for each set. There were six conditions for selecting the number of training and testing samples. The accuracy of the classification with a certain condition with five types of (P, R) varying from (8, 1) to (24, 3). The obtained results with LBP and NN can be seen from Table 1.

Table 1 shows the results with classical LBP and NN. The radius value of R and the neighbourhood value of P are both effective on classification performance. Accordingly, the best classification accuracy of 98.25 was recorded when 60% training and 40% testing samples were used and R and P values were set as

Table 2 Classification results with CNN

Training samples, %	Testing samples, %	Accuracy, %
10	90	98, 50
20	80	99, 60
30	70	99, 50
40	60	99, 80
50	50	99, 80
60	40	99, 40

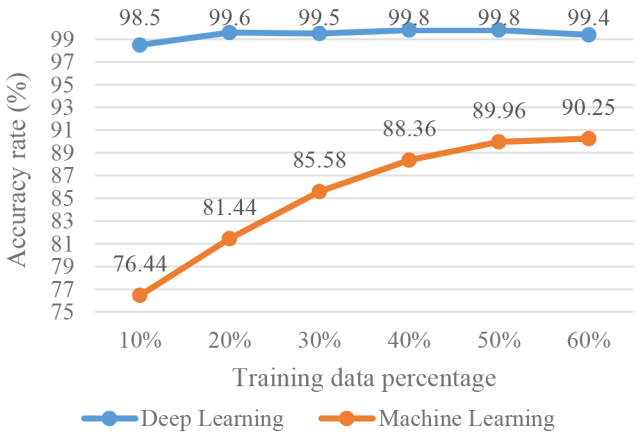

Fig. 7 *Comparison of CNN and NN*

3 and 16, respectively. The worst classification performance of 70.33 was obtained by using 10% training and 90% test samples due to the little number of samples. For the LBP values, if the *P*-value was selected high, feature dimension increases so it affects the classification performance. For LBP, classifier gives promising results whenever the testing samples decrease.

For the evaluation process of the deep learning method performance, CNN was applied on light microscopy images. The test and training sets were selected randomly which are 882 mohair and 864 wool. The experimental procedure is as follows: all samples were obtained under the same condition and separated into training and testing samples with the aim of evaluation. Training and testing sets were selected randomly in each class. There were six conditions for selecting the number of training and testing samples. Table 2 shows the obtained results with deep learning.

Fig. 7 shows the comparison of CNN and NN results graphically.

It can be seen that when the training data percentage increases the classification accuracy also increases with NN. For CNN structure, the classification performance gives promising results for all percentage of the training set.

The classification accuracy of the proposed method was compared with those of the state-of-the-art texture descriptors using the same classifier from the literature which is illustrated in Table 3. The results of the proposed method were compared with the results from literature related to the animal-based fibres. Accordingly, in [3], the cashmere and wool fibre properties have been obtained by RILBP and classified by SVM with a 90% accuracy. In [12], the mohair and merino fibres have been classified by hybrid ANN (HANN) with a 96.35% accuracy. Cashmere and wool fibres have been distinguished by using Bayes classifier with a 90% accuracy [22]. Cashmere and wool fibres are classified with SVM using bag of words and spatial pyramid match. The results show that the identification accuracy of each data set exceeded 90% [39]. Xing *et al.* have been proposed a method which is based on histogram of oriented gradient (HOG) with SVM. The experimental results have shown that the recognition accuracy of the fibre images was found with the highest value of 92.50% [40]. Sun *et al.* have designed a novel identification method combining NIR and nearest regularization subspace. The performance of the classification has been compared with two methods namely SVM and soft independent modelling by class analogy (SIMCA). The classification accuracy has been

Table 3 Classification accuracy of the proposed method and state-of-the-art methods

Various methods	Classification accuracy, %
SVM [3]	90.00
HANN [12]	96.35
SVM [39]	90.00
Bayes [22]	90.00
HOG + SVM [40]	92.50
SVM&SIMCA [41]	93.33
SVM [42]	93.00
MLP [43]	96.00
CNN [44]	95.20
CNN (proposed)	99.80

recorded as 93.33% [41]. Lu *et al.*have been proposed speed up robust features based SVM classification method for separating the cashmere and wool fibres. Scanning electron microscopy images have been used for getting images of fibres. The results have shown that the recognition rate has been found to be >93% [42]. Wang has proposed a new identification algorithm which extracts the information about fibre with the adaptive threshold and Hough transform. MLP has been used for classification part. Experiments have shown that the proposed method can obtain a 96% accuracy on the data sets [43]. Wang and Jin have stated CNN to classify wool and cashmere fibre images. The model has been used as a part level feature to enhance the object level features for classification. The best accuracy obtained is 95.20% [44]. In this study, the classification of wool and mohair fibres were performed by using CNN. The performance of the presented study with a 99.8% accuracy is comparable considering the related state-of-the-art studies.

4 Conclusion

In this study, the identification and classification processes of wool and mohair fibres were performed. For this purpose, two different methods were employed. First one LBP was used for texture feature extraction process and NN algorithm was used for classification. The second one CNN was used for the classification process. By using numerous training and test data sets, the proposed system was examined and around 98% accuracy was obtained with CNN. Compared to the commonly used methods, such as image recognition that is based on samples collected with scanning electron microscope, the proposed method shortens the processing time involved in complicated processes of scanning electron microscope. Additionally, it serves in an alternative way with higher accuracy by saving both time and labour in comparison with the non-automatic classification methods. Also training and test samples can be increased to improve the precision of the study. As a future work and continuation of this project, different algorithms like *R*-CNN, Fast *R*-CNN and Faster *R*-CNN will be investigated and tried for implementation. Furthermore, one of the goals is to create and train custom model from scratch rather than using pre-trained model. Training model from scratch will allow to have control over the whole training process even feature learning part which contains pooling and activation processes. Besides, studies will also be in the way of searching better classifier techniques.

5 References

[1] Fujishige, S., Koshiba, Y.: 'Identifying cashmere and merino wool fibers', *Tex. Res. J.*, 1997, **67**, (8), pp. 619–620

[2] He, L. Z., Chen, L. P., Wang, X. M.: 'Detection methods of distinguishing cashmere and wool fibers', *Prog. Tex. Sci. Technol.*, 2008, **2**, pp. 64–65

[3] Lu, K., Chai, X., Xie, H., *et al.*: 'Identification of cashmere/wool based on pairwise rotation invariant co-occurrence local binary pattern'. Int. Conf. on Computational Science and Computational Intelligence (CSCI), Las Vegas, NV, USA, Dec 2017, pp. 463–467

[4] Van Niekerk, W. A., Keva, S., Roets, M., *et al.*: 'The accuracy of video image analysis (VIA) and optical fibre diameter analysis (OFDA) to measure fibre diameter of cashmere', *S. Afr. J. Anim. Sci.*, 2004, **34**, (5), pp. 143–144

[5] Yuan, S., Lu, K., Zhong, Y.: 'Identification of wool and cashmere based on texture analysis', *Key Eng. Mater.*, 2016, **671**, pp. 385–390

[6] Guifen, Y., Yan, F., Xia, H., *et al.*: 'Discussion on the SEM/OM in cashmere identification', *China Fiber Insp.*., 2006, **6**, pp. 17–20

[7] Nelson, G., Hamlyn, P. F., Holden, L., *et al.*: 'A species-specific DNA probe for goat fiber identification', *Tex. Res. J.*, 1992, **62**, (10), pp. 590–595

[8] Wu, G. F., Zhu, D. S., He, Y.: 'Identification of fine wool and cashmere by using Vis/NIR spectroscopy technology'. Int. Symp. on Photoelectronic Detection and Imaging: Technology and Applications, Beijing, China, Feb 2008, pp. 1260–1263

[9] Zhi-ming, Z.: 'Study on quick test of blend ratio of cashmere and wool with computer', *Wool Tex. J.*, 2005, **10**, pp. 44–46

[10] Robson, D.: 'Animal fiber analysis using imaging techniques part I: scale pattern data', *Tex. Res. J.*, 1997, **67**, (10), pp. 747–752

[11] She, F., Chow, S., Wang, B., *et al.*: 'Identification and classification of animal fibres using artificial neural networks', *J. Tex. Eng.*, 2001, **47**, (2), pp. 35–38

[12] Kong, L. X., She, F. H., Nahavandi, S., *et al.*: 'Fuzzy pattern recognition and classification of animal fibers'. Joint 9th IFSA World Congress and 20th NAFIPS Int. Conf., Vancouver, BC, Canada, July 2001, pp. 1050–1055

[13] Zhong, Y., Lu, K., Tian, J., *et al.*: 'Wool/cashmere identification based on projection curves', *Tex. Res. J.*, 2016, **87**, (14), pp. 1730–1741

[14] Xing, W., Deng, N., Xin, B., *et al.*: 'Investigation of a novel automatic micro image-based method for the recognition of animal fibers based on wavelet and Markov random field', *Micron*, 2019, **119**, pp. 88–97

[15] Xing, W., Deng, N., Xin, B., *et al.*: 'An image-based method for the automatic recognition of cashmere and wool fibers', *Measurement*, 2019, **141**, pp. 102–112

[16] Zhang, J., Palmer, S., Wang, X.: 'Identification of animal fibers with wavelet texture analysis'. Proc. of the World Congress on Engineering, London, England, Jun 2010, pp. 742–747

[17] Xing, W., Xin, B., Deng, N., *et al.*: 'A novel digital analysis method for measuring and identifying of wool and cashmere fibers', *Measurement*, 2019, **132**, pp. 11–21

[18] Zhang, Z., Ren, J., Li, S., *et al.*: 'Robust subspace discovery by block-diagonal adaptive locality-constrained representation', Proc. 27th ACM International Conference on Multimedia, Nice, France, 2019, pp. 1569–1577

[19] Kong, L., She, F. H., Nahavandi, S., *et al.*: 'Feature extraction for animal fiber identification'. Second Int. Conf. on Image and Graphics, Hefei, China, July 2002, pp. 699–704

[20] Zhang, Z., Li, F., Zhao, M., *et al.*: 'Robust neighborhood preserving projection by nuclear/L2, 1-norm regularization for image feature extraction', *IEEE Trans. Image Process.*, 2017, **26**, (4), pp. 1607–1622

[21] Zhang, Z., Li, F., Zhao, M., *et al.*: 'Joint low-rank and sparse principal feature coding for enhanced robust representation and visual classification', *IEEE Trans. Image Process.*, 2016, **25**, (6), pp. 2429–2443

[22] Shi, X.-J., Yu, W.-D.: 'Identification of animal fiber based on scale shape'. Congress on Image and Signal Processing, Sanya, Hainan, China, May 2008, pp. 573–577

[23] Ojala, T., Pietikäinen, M., Harwood, D.: 'A comparative study of texture measures with classification based on featured distributions', *Pattern Recognit.*, 1996, **29**, (1), pp. 51–59

[24] Ojala, T., Pietikainen, M., Maenpaa, T.: 'Multiresolution gray-scale and rotation invariant texture classification with local binary patterns', *IEEE Trans. Pattern Anal. Mach. Intell.*, 2002, **24**, (7), pp. 971–987

[25] Caputo, B., Hayman, E., Mallikarjuna, P.: 'Class-specific material categorisation'. Tenth IEEE Int. Conf. on Computer Vision (ICCV'05) Volume 1, Beijing, China, Oct 2005, pp. 1597–1604

[26] Ahonen, T., Pietikäinen, M.: 'Soft histograms for local binary patterns'. Proc. Finnish Signal Processing Symp., Oulu, Finland, 2007, p. 1

[27] Ahonen, T., Pietikäinen, M.: 'Image description using joint distribution of filter bank responses', *Pattern Recognit. Lett.*, 2009, **30**, (4), pp. 368–376

[28] Liao, S., Law, M. W. K., Chung, A. C. S.: 'Dominant local binary patterns for texture classification', *IEEE Trans. Image Process.*, 2009, **18**, (5), pp. 1107–1118

[29] Guo, Z., Zhang, L., Zhang, D.: 'A completed modeling of local binary pattern operator for texture classification', *IEEE Trans. Image Process.*, 2010, **19**, (6), pp. 1657–1663

[30] Liao, W.-H., Young, T.-J.: 'Texture classification using uniform extended local ternary patterns'. IEEE Int. Symp. on Multimedia, Taichung, Taiwan, Dec 2010, pp. 191–195

[31] Liu, L., Zhao, L., Long, Y., *et al.*: 'Extended local binary patterns for texture classification', *Image Vis. Comput.*, 2012, **30**, (2), pp. 86–99

[32] LeCun, Y., Bottou, L., Bengio, Y., *et al.*: 'Gradient-based learning applied to document recognition', *Proc. IEEE*, 1998, **86**, (11), pp. 2278–2324

[33] Hubel, D. H., Wiesel, T. N.: 'Receptive fields and functional architecture of monkey striate cortex', *J. Physiol.*, 1968, **195**, (1), pp. 215–243

[34] Ren, R., Hung, T., Tan, K. C.: 'A generic deep-learning-based approach for automated surface inspection', *IEEE Trans. Cybern.*, 2018, **48**, (3), pp. 929–940

[35] Schmidhuber, J.: 'Deep learning in neural networks: an overview', *Neural Netw.*, 2015, **61**, pp. 85–117

[36] Krizhevsky, A., Sutskever, I., Hinton, G. E.: 'Imagenet classification with deep convolutional neural networks'. Advances in Neural Information Processing Systems, Lake Tahoe, Nevada, Dec 2012, pp. 1097–1105

[37] Sermanet, P., Eigen, D., Zhang, X., *et al.*: 'Overfeat: integrated recognition, localization and detection using convolutional networks'. Int. Conf. on Learning Representations, Banff, Canada, Apr 2014

[38] Donahue, J., Jia, Y., Vinyals, O., *et al.*: 'Decaf: a deep convolutional activation feature for generic visual recognition'. Int. Conf. on machine learning, Beijing, China, June 2014, pp. 647–655

[39] Lu, K., Zhong, Y., Li, D., *et al.*: 'Cashmere/wool identification based on bag-of-words and spatial pyramid match', *Tex. Res. J.*, 2018, **88**, (21), pp. 2435–2444

[40] Xing, W., Deng, N., Xin, B., *et al.*: 'Identification of extremely similar animal fibers based on matched filter and HOG-SVM', *IEEE. Access.*, 2019, **7**, pp. 98603–98617

[41] Sun, X., Yuan, H., Song, C., *et al.*: 'A novel drying-free identification method of cashmere textiles by NIR spectroscopy combined with an adaptive representation learning classification method', *Microchem. J.*, 2019, **149**, p. 104018

[42] Lu, K., Luo, J., Zhong, Y., *et al.*: 'Identification of wool and cashmere SEM images based on SURF features', *J. Eng. Fibers Fabr.*, 2019, **14**, doi:10.1177/1558925019866121

[43] Wang, H.: 'Combining the Hough transform with MLP for identifying cashmere and wool fibers'. Proc. of the 2019 5th Int. Conf. on Computer and Technology Applications, Istanbul, Turkey, 2019, pp. 124–128

[44] Wang, F., Jin, X.: 'The application of mixed-level model in convolutional neural networks for cashmere and wool identification', *Int. J. Cloth. Sci. Technol.*, 2018, **30**, (5), pp. 710–725